

Preparation and characterization of new Mn₆ and Mn₈ clusters obtained from the *in situ* formation of an unprecedented octadentate ligand

Theocharis C. Stamatatos, Khalil A. Abboud, George Christou *

Department of Chemistry, University of Florida, Gainesville, FL 32611-7200, USA

ARTICLE INFO

Article history:

Received 29 January 2008
Received in revised form 6 April 2008
Accepted 7 April 2008
Available online 24 April 2008

Keywords:

Crystal structures
1,3,5-Trihydroxybenzene
Magnetochemistry
Manganese propionate chemistry
Mixed-valence manganese clusters

ABSTRACT

The use of 1,3,5-trihydroxybenzene (thbH₃) in manganese carboxylate chemistry has been investigated. The reactions of thbH₃ with 4 and 6 equivalents of Mn(O₂CET)₂ in MeOH afford the complexes [Mn₆(O₂-CET)₈(L)(MeOH)₄(H₂O)₂] (**1**) and [Mn₈O₂(O₂CET)₁₄(MeOH)₄] (**2**), respectively. In the case of complex **1**, the product of the *in situ* organic ligand transformation has been observed, namely the conversion of the tridentate thbH₃ group to a new octadentate ligand L⁴⁻; the latter has never been previously reported. Both complexes possess rare topologies, with **1** containing 6Mn^{II} ions, whereas **2** is mixed-valent 6Mn^{II}, 2Mn^{III}. The core of **1** consists of two [Mn₃(μ₃-OR)]⁵⁺ triangles linked by the bulky octadentate ligand L. The [Mn₈(μ₄-O)₂(μ-OR)₈]⁶⁺ core of **2** can be considered an extension of the common [Mn₆(μ₄-O)₂]¹⁰⁺ (4Mn^{II}, 2Mn^{III}) core, comprising two edge-sharing tetrahedra, with two additional Mn atoms at one end. Peripheral ligation in both **1** and **2** is provided by eight and fourteen bridging EtCO₂⁻ groups, respectively. Variable-temperature, solid-state dc and ac magnetization studies were carried out on complexes **1** and **2** in the 1.8–300 K range. The magnetic susceptibility data for **1** were fit to the theoretical χ_M vs T expression, derived by the use of an isotropic Heisenberg spin Hamiltonian and the Van Vleck equation, for two essentially non-interacting triangular [Mn₃(μ₃-OR)(μ-OR)₂]³⁺ units. The fitting procedure revealed the two pairwise exchange parameters to be weakly ferromagnetic ($J_{\text{basal}} = J' = +0.79(3) \text{ cm}^{-1}$) and antiferromagnetic ($J_{\text{side}} = J = -2.04(3) \text{ cm}^{-1}$), respectively, resulting in an $S = 5/2$ spin ground state. In contrast, the data for **2** revealed dominant antiferromagnetic interactions and a resulting $S = 0$ ground state; the latter value is rationalized in terms of the strong antiferromagnetic coupling within the central Mn^{III}O₂ unit.

© 2008 Elsevier B.V. All rights reserved.

1. Introduction

The continuing interest in the synthesis and characterization of polynuclear manganese carboxylate complexes in intermediate oxidation states has three main driving forces: (i) the desire to recreate with synthetic models the structure, spectroscopic properties and/or function of the active sites of several redox enzymes containing a carboxylate-bridged manganese core; the most fascinating of these is the water-oxidizing complex (WOC) of green plants and cyanobacteria, which is a Mn₄Ca complex [1]; (ii) the realization that oligo- and polynuclear Mn carboxylate compounds containing Mn^{III} atoms often have large, and sometimes abnormally large, ground state spin (S) values as a result of ferromagnetic exchange interactions and/or spin frustration effects, which combined with a large and negative magnetoanisotropy (as reflected in a large and negative zero-field splitting parameter, D) have led to some of these species having a significant energy barrier (vs kT , where k is the Boltzmann constant) to magnetization relaxation and thus functioning as single-molecule magnets

(SMMs) [2,3]; and (iii) the ability of high-oxidation state molecular compounds or polymeric oxides of Mn to oxidize both inorganic and organic substrates, which have led to a wide range of catalytic applications in diverse areas involving inorganic, organic, environmental, and industrial chemistry [4].

Progress in the field of high-spin molecules and the chances of identifying new SMMs will both benefit from the development of new synthetic methodologies to Mn carboxylate clusters [5]. Discovering new preparative routes is thus of great interest not only for the isolation of completely new complexes but also as a means of building up families of related Mn carboxylate species so that structure–property relations can be developed. The choice of ligands in such studies is obviously crucial, because the versatility, flexibility, chelate bite size(s) and other ligand properties are of great importance in determining the structure of the product.

One synthetic methodology that has proven to be very useful for the synthesis of new polynuclear Mn complexes is the reaction of a chelating ligand with simple Mn carboxylate sources, e.g. Mn(O₂CR)₂ (R = Me, Et and Ph), or with a preformed Mn carboxylate cluster that does not already contain any chelating ligands [6]. Chelates that have previously proven useful are, amongst others, 2,2'-bipyridine [7], 2-picolinate [8] and the anion of dibenzoylmethane

* Corresponding author. Tel.: +1 352 392 6737; fax: +1 352 392 8757.
E-mail address: christou@chem.ufl.edu (G. Christou).

[9]. Thus, for example, the reaction of 2,2'-bipyridine (bpy) with $[\text{Mn}_3\text{O}(\text{O}_2\text{CR})_6(\text{py})_3]^+$ was the original way by which the tetranuclear “butterfly” complexes $[\text{Mn}_4\text{O}_2(\text{O}_2\text{CR})_7(\text{bpy})_2]^+$ were obtained [7a].

As part of this work, we have also explored a wide variety of new potentially chelating and/or bridging ligands that might foster formation of high nuclearity Mn products. One such family is the alkoxide-based chelates, which includes pyridyl alcohols [10], diols [11], and triols [12], amongst others [13]. All of these ligands have proved to be extremely versatile chelating and bridging groups that have yielded a number of 3d metal clusters with various structural motifs, large *S* values, and SMM behaviors. More recently, we have been investigating a number of other O-based alcohol ligands, and one of these has been the phenol (PhOH; Fig. 1). We recently reported, for example, the employment of PhOH in Fe carboxylate chemistry, which gave the octanuclear “ferric wheel” complexes $[\text{Fe}_8(\text{OH})_4(\text{OPh})_8(\text{O}_2\text{CR})_{12}]$ [14]. As an extension to this work with PhOH, we have now asked what kind of products might result from the addition of two more alcohol arms onto the PhOH group but on the *meta*-sides (3 and 5 positions) of the phenol ring; the resulting molecule, 1,3,5-trihydroxybenzene (thbH₃), is shown in Fig. 1. We anticipated that the use of thbH₃ triol in polynuclear transition metal cluster chemistry would give products distinctly different from those with simple phenols (i.e. PhOH), and we have therefore explored its use in Mn chemistry. Note that thbH₃ has never been previously employed in coordination chemistry with any metal. In the present investigation, we have deliberately targeted high nuclearity Mn products by exploring the reactions between thbH₃ and various Mn carboxylate starting materials under ambient conditions. This has successfully led to Mn₆ and Mn₈ carboxylate cluster products containing, in the former case, the tetraanion of an unprecedented organic ligand (L^{4-} ; Fig. 1), which resulted from the *in situ* structural transformation of the thbH₃ molecule. The syntheses, structures, and magnetochemical characterization of these complexes are described in this paper.

2. Experimental

2.1. General and physical measurements

All manipulations were performed under aerobic conditions using chemicals and solvents as received, unless otherwise stated. $\text{Mn}(\text{O}_2\text{Cet})_2 \cdot x\text{H}_2\text{O}$ was prepared as described elsewhere [15].

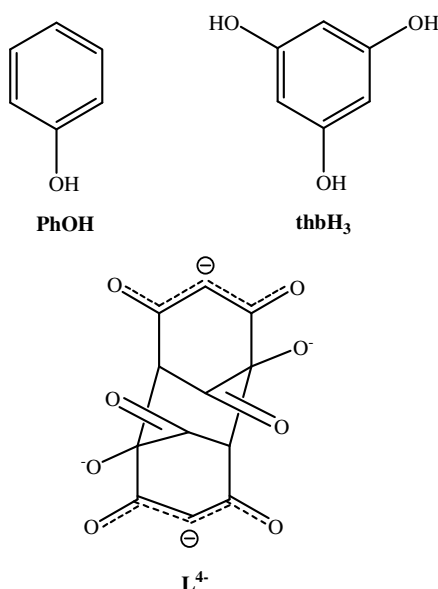


Fig. 1. The ligands discussed in this work.

Infrared spectra were recorded in the solid-state (KBr pellets) on a Nicolet Nexus 670 FTIR spectrometer in the 400–4000 cm^{-1} range. Elemental analyses (C, H and N) were performed by the in-house facilities of the University of Florida Chemistry Department. Variable-temperature dc and ac magnetic susceptibility data were collected at the University of Florida using a Quantum Design MPMS-XL SQUID susceptometer equipped with a 7 T magnet and operating in the 1.8–300 K range. Samples were embedded in solid eicosane to prevent torquing. Pascal's constants were used to estimate the diamagnetic corrections, which were subtracted from the experimental susceptibilities to give the molar paramagnetic susceptibilities (χ_M).

2.2. Compound preparation

2.2.1. $[\text{Mn}_6(\text{O}_2\text{Cet})_8(\text{L})(\text{MeOH})_4(\text{H}_2\text{O})_2]$ (**1**)

A pink solution of $\text{Mn}(\text{O}_2\text{Cet})_2 \cdot x\text{H}_2\text{O}$ (0.40 g, 2.0 mmol) in MeOH (20 mL) was treated with solid thbH₃ (0.05 g, 0.5 mmol). The solid soon dissolved, and the resulting pale yellow solution was stirred for about 1 h, during which time the reaction mixture colour changed from pale yellow to orange. The solution was filtered, and the filtrate left undisturbed to concentrate slowly by evaporation. After five days, large pale orange crystals of **1** were collected by filtration, washed with cold MeOH (2×3 mL) and Et₂O (2×5 mL), and dried in air. Yield: 60% (based on the total available Mn). The dried sample analysed as solvent-free. *Anal. Calc.* for $\text{C}_{40}\text{H}_{64}\text{O}_{30}\text{Mn}_6$: C, 35.47; H, 4.76. Found: C, 35.39; H, 4.58%. Selected IR data (KBr pellet, cm^{-1}): 3221m, 2979m, 1714m, 1536s, 1465m, 1412s, 1302m, 1226m, 1144m, 1078m, 1024m, 889w, 815m, 635m, 442w.

2.2.2. $[\text{Mn}_8\text{O}_2(\text{O}_2\text{Cet})_{14}(\text{MeOH})_4]$ (**2**)

Method A. A pink solution of $\text{Mn}(\text{O}_2\text{Cet})_2 \cdot x\text{H}_2\text{O}$ (0.60 g, 3.0 mmol) in MeOH (20 mL) was treated with solid thbH₃ (0.05 g, 0.5 mmol). The solid soon dissolved, and the resulting pale yellow solution was stirred for about 1 h, during which time the reaction mixture colour changed from pale yellow to deep orange. The solution was filtered, and the filtrate was layered with Me₂CO (40 mL). After 10 days, dark orange crystals of **2** were collected by filtration, washed with cold Me₂CO (2×3 mL) and Et₂O (2×5 mL), and dried in air. Yield: 45% (based on the total available Mn). The dried sample analysed as solvent-free. *Anal. Calc.* for $\text{C}_{46}\text{H}_{86}\text{O}_{34}\text{Mn}_8$: C, 34.05; H, 5.34. Found: C, 32.89; H, 5.41%. Selected IR data (KBr pellet, cm^{-1}): 3213m, 2965m, 1535s, 1361m, 1300m, 1272m, 1235m, 1198m, 1047m, 966m, 934m, 906m, 806m, 772w, 733s, 639m, 606s, 579m, 519w, 475m, 449w, 416w.

Method B. A pink solution of $\text{Mn}(\text{O}_2\text{Cet})_2 \cdot x\text{H}_2\text{O}$ (0.60 g, 3.0 mmol) in MeOH (20 mL) was stirred for about 6 h, during which time the reaction mixture colour changed to deep orange. The solution was filtered, and the filtrate was layered with Me₂CO (40 mL). After six days, dark orange crystals of **2** were collected by filtration, washed with cold Me₂CO (2×3 mL) and Et₂O (2×5 mL), and dried in air. Yield: 70% (based on the total available Mn). The identity of the product was confirmed by elemental analysis (C, H and N) and IR spectroscopic comparison with material from Method A.

2.3. Single-crystal X-ray crystallography

Data were collected on a Siemens SMART PLATFORM equipped with a CCD area detector and a graphite monochromator utilizing MoK α radiation ($\lambda = 0.71073$ Å). Suitable crystals of **1** and **2** were attached to glass fibers using silicone grease and transferred to a goniostat where they were cooled to 173 K for data collection. An initial search for reciprocal space revealed a monoclinic cell for **1**, and an orthorhombic cell for **2**; the choice of space groups $C2/c$

(for **1**) and *Pna2*₁ (for **2**) was confirmed by the subsequent solution and refinement of the structures. Cell parameters were refined using up to 8192 reflections. A full sphere of data (1850 frames) was collected using the ω -scan method (0.3° frame width). The first 50 frames were re-measured at the end of data collection to monitor instrument and crystal stability (maximum correction on *I* was <1%). Absorption corrections by integration were applied based on measured indexed crystal faces. The structures were solved by direct methods in *SHELXTL6* [16], and refined on *F*² using full-matrix least-squares. The non-H atoms were treated anisotropically, whereas the H atoms were placed in calculated, ideal positions and refined as riding on their respective C atoms. Unit cell parameters and structure solution and refinement data are listed in Table 1.

For **1**, the asymmetric unit consists of half the Mn₆ cluster located on an inversion centers. There are three disordered propionates, one disordered methanol, and one disordered coordinated water molecule. All disorders were refined in two parts, each with their site occupation factors dependently refined. A total of 340 parameters were included in the structure refinement using 18509 reflections with *I* > 2σ(*I*) to yield *R*₁ and *wR*₂ of 6.14% and 12.84%, respectively.

For **2**, the asymmetric unit contains the complete Mn₈ cluster. Four propionate ligands have their methyl groups disordered and were refined in two parts each with their site occupation factors at 0.7/0.3 or 0.6/0.4. A total of 32728 parameters were included in the structure refinement using 817 reflections with *I* > 2σ(*I*) to yield *R*₁ and *wR*₂ of 6.23% and 12.17%, respectively.

3. Results and discussion

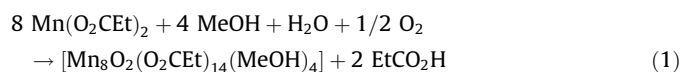
3.1. Syntheses

As stated above, many synthetic procedures to polynuclear manganese carboxylate clusters rely on the reaction of simple Mn^{II} salts, such as Mn(O₂CR)₂ (R = various) or preformed higher oxidation state Mn_x clusters, i.e. triangular [Mn₃O(O₂CR)₆L₃]^{0/+} species, with a potentially chelating/bridging ligand [6]. Both of these strategies have previously proved to be useful routes to a variety of

higher-nuclearity complexes with ligands ranging from bidentate to pentadentate [10–13]. The present study employed the former strategy with the potentially tridentate ligand thbH₃. Thus, a variety of reaction ratios and solvents, carboxylate reagents, and other conditions were investigated. The reaction of thbH₃ with four equivalents of Mn(O₂CET)₂ in MeOH afforded a pale orange solution from which was subsequently obtained the hexanuclear complex [Mn₆(O₂CET)₈(L)(MeOH)₄(H₂O)₂] (**1**) in ~60% yield. Complex **1** was also obtained, but in lower yields of 10–30%, from the reaction of thbH₃ with 1–3 equivalents of Mn(O₂CET)₂ in MeOH. We also investigated the identity of the product as a function of the carboxylate groups on the Mn^{II} starting material, but we were unable to isolate pure, crystalline materials for satisfactory characterization. The use of other alcohols such as EtOH and PrⁿOH, or a non-alcohol such as MeCN or CH₂Cl₂, as reaction solvent gave only insoluble, amorphous precipitates that we were not able to characterize further. The presence of counter-cations or -anions, and/or the presence of extra inorganic anions with coordinating affinity (i.e. Cl⁻, N₃⁻, etc...) had no influence on the identity of the product. Attempts to oxidize one or more Mn^{II} ions of **1** failed to give a crystalline compound. Several 1/NBu₄⁺MnO₄⁻ reaction mixtures, and *in situ* reactions between Mn(O₂CET)₂ and thbH₃ in the presence of NBu₄⁺MnO₄⁻ at various Mn^{II}/Mn^{VII} ratios were studied using different conditions, but almost all led to dark brown amorphous precipitates; we did not study these materials further.

The most remarkable feature of the reaction that led to complex **1** is the *in situ* transformation of the tridentate ligand thbH₃ to the tetraanion of an unprecedented octadentate ligand L⁴⁻ (Fig. 1), most probably from a complicated redox reaction of two thbH₃ molecules with the reaction solvent MeOH (and/or H₂O) and air, in the presence of the Mn²⁺ cations. A search of the chemical literature reveals that no organic compound structurally similar (or even related) to L⁴⁻ has been reported to date. As a consequence, an extensive search of the Cambridge Crystallographic Database did not locate any crystal structures of metal compounds containing L⁴⁻ as a ligand. The mechanism of this transformation is clearly very complicated and we refrain from unnecessary speculation (*vide infra*).

When more than four equivalents of Mn(O₂CET)₂ were employed in reactions with thbH₃ in MeOH, the colour of the solution become dark orange (compared to the solution of complex **1**), and subsequently gave dark orange crystals of the octanuclear, thbH₃-free, complex [Mn₈O₂(O₂CET)₁₄(MeOH)₄] (**2**) in ~45% yield. Complex **2** was also obtained, and in a higher yield of 70%, from the simple dissolution of Mn(O₂CET)₂ in MeOH, and subsequent crystallization (Method B). The compound is mixed-valent, containing six Mn^{II} and two Mn^{III} ions. Given that the starting manganese source contains only Mn^{II} ions, it is clear that the Mn^{III} ions are formed by aerial oxidation during the extensive stirring time, as observed by the colour change from pink to dark orange. As is almost always the case in Mn cluster chemistry, the mechanism of formation is likely to be complicated, involving the protonation/deprotonation, oxidation/reduction and structural rearrangement of several species in solution, and thus a mechanistic rationalization is not possible. The formation of complex **2** is summarized in Eq. (1).



We again investigated the identity of the product as a function of the carboxylate groups on the Mn^{II} starting material, but obtained [Mn₈O₂(O₂CR)₁₄(L')₄] (R = Me, Bu^t, CH₂Bu^t; L' = terminally ligated groups) products isostructural to **2** with identical magnetic properties (*vide infra*). Clearly, the core of complex **2** is the preferred product of these reaction components under these conditions. However,

Table 1
Crystallographic data for complexes **1** and **2**

Parameter	1	2
Formula	C ₄₀ H ₆₄ Mn ₆ O ₃₀	C ₄₆ H ₈₆ Mn ₈ O ₃₄
Formula weight	1354.55	1622.67
Crystal system	Monoclinic	Orthorhombic
Space group	<i>C2/c</i>	<i>Pna2</i> ₁
<i>Unit cell dimensions</i>		
<i>a</i> (Å)	15.9148(17)	26.823(2)
<i>b</i> (Å)	21.837(2)	11.3028(9)
<i>c</i> (Å)	16.1832(16)	23.3933(18)
β (°)	97.124(2)	90
<i>V</i> (Å ³)	5580.6(2)	7092.2(2)
<i>Z</i>	4	4
ρ_{calc} (g cm ⁻³)	1.612	1.520
Radiation, λ (Å)	MoK α , 0.71073	MoK α , 0.71073
Temperature (K)	173(2)	173(2)
μ (mm ⁻¹)	1.404	1.458
Reflections collected/unique (<i>R</i> _{int})	18509/6363(0.0945)	32728/10592(0.1159)
Data with <i>I</i> > 2σ(<i>I</i>)	3311	7289
Parameters refined	340	817
($\Delta\rho$) _{max} , ($\Delta\rho$) _{min} (e Å ⁻³)	0.606, -0.349	0.469, -0.483
Goodness-of-fit (on <i>F</i> ²)	0.999	1.032
<i>R</i> ₁ ^a , <i>wR</i> ₂ ^b (all data)	0.1381, 0.1643	0.1086, 0.1428
<i>R</i> ₁ ^a , <i>wR</i> ₂ ^b (<i>I</i> > 2σ(<i>I</i>))	0.0614, 0.1284	0.0623, 0.1217

^a *R*₁ = Σ(|*F*_o - *F*_c|)/Σ(|*F*_o|).

^b *wR*₂ = [Σ(w(*F*_o² - *F*_c²)²)/Σ(w(*F*_o²)²)]^{1/2}, $w = 1/[\sigma^2(F_o^2) + (ap)^2 + bp]$, where $p = [\max(F_o^2, 0) + 2F_c^2]/3$.

with R = Ph, a different product was isolated, namely the hexanuclear mixed-valent $[\text{Mn}_6\text{O}_2(\text{O}_2\text{CPh})_{10}(\text{HO}_2\text{CPh})_2(\text{H}_2\text{O})_2]$ (**3**) complex with the common $\{\text{Mn}_4^{\text{II}}\text{Mn}_2^{\text{III}}\text{O}_2\}^{10+}$ core and an $S = 0$ spin ground state value.

3.2. Description of structures

A partially labeled representation and a stereoview of complex **1** are shown in Fig. 2. Selected interatomic distances and angles are listed in Table 2. Complex **1** crystallizes in monoclinic space group $C2/c$ and possesses crystallographic C_2 symmetry. The core of **1** consists of six Mn ions arranged as a dimer of two $[\text{Mn}_3(\mu_3\text{-OR})]^{5+}$ triangles linked together by the bulky octadentate ligand L (Fig. 3). Each $[\text{Mn}_3(\mu_3\text{-OR})]^{5+}$ triangular unit is essentially isosceles within the usual 3σ criterion ($\text{Mn1}\cdots\text{Mn2} = 3.554(2)$ Å, $\text{Mn1}\cdots\text{Mn3} = 3.539(2)$ Å, $\text{Mn2}\cdots\text{Mn3} = 3.083(2)$ Å), and non-planar. The central μ_3 -alkoxide atom O1 is 1.037 Å above the Mn_3 plane and has distorted tetrahedral geometry. The $\text{Mn}-\mu_3\text{-OR}^--\text{Mn}$ angles range from $86.76(12)^\circ$ to $107.06(14)^\circ$, deviating significantly from the 109.5° ideal values of a tetrahedron, whereas the three $\text{Mn}-\text{OR}^-$ bonds are also distinctly different (2.196(3)–2.265(4) Å). The two equivalent basal sides ($\text{Mn2}\cdots\text{Mn3}$) of each isosceles triangle are additionally bridged by two monoatomic $\mu\text{-O}$ atoms (O21, O31) of two EtCO_2^- groups, with their second O atoms being either dangling (O22) or bridging (O32) to an adjacent Mn atom (Mn1), respectively. Thus, two of the carboxylato groups are arranged in the fairly rare $\eta^1:\eta^2:\mu_3$ mode, whereas the other two are in the more usual $\eta^2:\mu$ mode. The complex therefore contains a $\{[\text{Mn}_3(\mu_3\text{-OR})(\mu\text{-OR})_2]\text{-L}[\text{Mn}_3(\mu_3\text{-OR})(\mu\text{-OR})_2]\}^{4+}$ core (Fig. 3) with the ligand L providing a long intra-triangular ‘spacer’; the inter-triangular Mn \cdots Mn separations within the Mn_6 molecule are in the 7.781(2)–8.762(2) Å range.

Peripheral ligation is further provided by four EtCO_2^- groups bridging in their familiar $\text{syn},\text{syn}-\eta^1:\eta^1:\mu$ mode, and six terminal

Table 2
Selected interatomic distances (Å) and bond angles ($^\circ$) for complex **1**

Interatomic distances			
Mn(1)–Mn(2)	3.554(2)	Mn(2)–O(31)	2.207(4)
Mn(1)–Mn(3)	3.539(2)	Mn(2)–O(71)	2.095(9)
Mn(2)–Mn(3)	3.083(2)	Mn(3)–O(1)	2.265(4)
Mn(1)–O(1)	2.196(3)	Mn(3)–O(4)	2.117(3)
Mn(1)–O(3)	2.311(4)	Mn(3)–O(21)	2.227(4)
Mn(1)–O(12)	2.145(3)	Mn(3)–O(31)	2.217(3)
Mn(1)–O(32)	2.135(4)	Mn(3)–O(41)	2.086(4)
Mn(1)–O(42)	2.186(3)	Mn(3)–O(51)	2.116(4)
Mn(1)–O(61)	2.156(4)	C(1)–O(1)	1.423(8)
Mn(2)–O(1)	2.223(3)	C(3)–O(2)	1.235(6)
Mn(2)–O(2)	2.126(4)	C(4)–O(3)	1.195(6)
Mn(2)–O(11)	2.123(4)	C(5)–O(4)	1.248(6)
Mn(2)–O(21)	2.259(4)		
Bond angles			
Mn(1)–O(1)–Mn(2)	107.06(14)	O(12)–Mn(1)–O(42)	170.03(15)
Mn(1)–O(1)–Mn(3)	104.95(14)	O(1)–Mn(2)–O(71)	172.5(3)
Mn(2)–O(1)–Mn(3)	86.76(12)	O(2)–Mn(2)–O(31)	158.29(13)
Mn(2)–O(21)–Mn(3)	86.81(14)	O(11)–Mn(2)–O(21)	170.25(15)
Mn(2)–O(31)–Mn(3)	88.35(13)	O(1)–Mn(3)–O(51)	164.53(15)
O(1)–Mn(1)–O(61)	166.77(14)	O(4)–Mn(3)–O(31)	158.89(14)
O(3)–Mn(1)–O(32)	170.31(15)	O(21)–Mn(3)–O(41)	168.19(14)

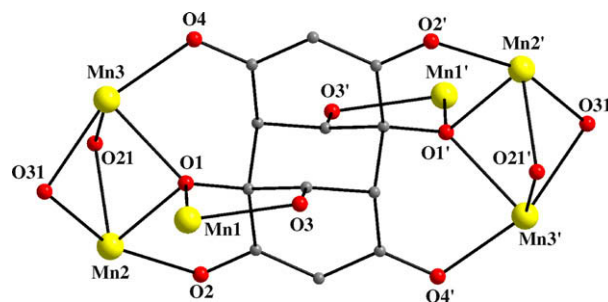


Fig. 3. PovRay representation of the labeled core of **1**. Color scheme: Mn^{II}, yellow; O, red; C, grey. (For interpretation of the references to colour in this figure legend, the reader is referred to the web version of this article.)

alkoxide arms from the ligand L. The ligation is completed by four terminally bound MeOH groups (O51, O61 and their symmetry-related partners) and two terminal H₂O molecules (O71, and its symmetry-related partner), each bound to a different Mn ion. All the Mn atoms are six-coordinate with distorted octahedral geometries. The oxidation states of all Mn atoms were established as +2 by charge balance considerations and inspection of Mn–O bond distances, and confirmed quantitatively by bond valence sum (BVS) calculations (Table 3) [17]. The protonation levels of the O atoms of the dangling EtCO_2^- and the ligand L were also confirmed by inspection of C–O bond distances and BVS calculations (Table 3). Given the overall charge of the Mn_6^{II} cluster, the octadentate ligand L should have a 4– charge. Taking into account the μ_3 mode of two of the RO^- groups (O1, and its symmetry-related partner) of the ligand L, and therefore their undoubtedly negatively charged character, the remaining two negative charges were attributed to a charge-delocalization between the O2/O4' and O4/O2' pair of atoms within the two O–C–CH–C–O units (see Figs. 1 and 3). Such a closely related charge-delocalization situation between two O atoms has been previously reported in many $\text{Mn}^{\text{II}}/\text{acac}^-$ complexes (acac^- = the anion of acetylacetonate), possessing very similar Mn^{II}–O, C–O and C–C distances with that of **1** [18]. The remaining two terminally ligated O atoms (O3, and its symmetry-related partner) of the ligand L have a more pronounced ketone-character as reflected in the shorter C–O distance ($\text{C4}-\text{O3} = 1.195(6)$ Å, Fig. S1), thus leaving a neutral charge around them.

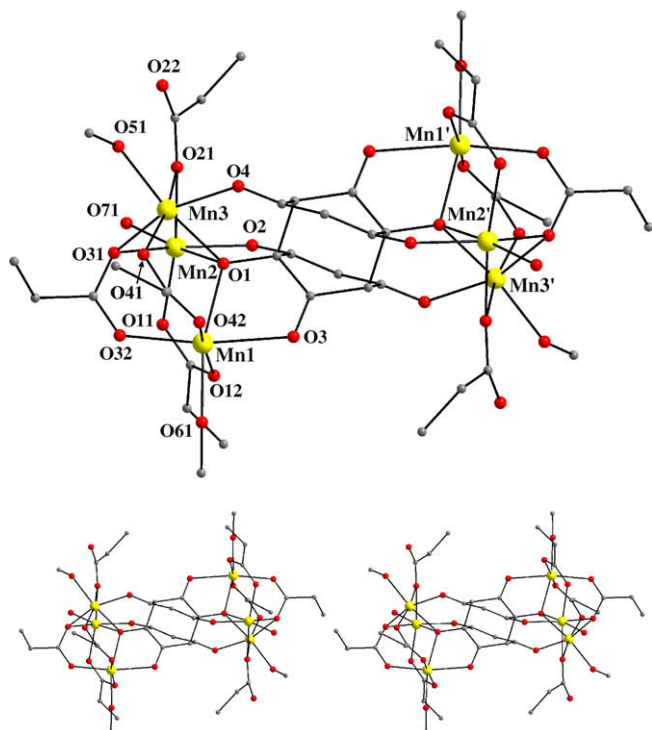


Fig. 2. Labeled PovRay representation (top) and stereopair (bottom) of complex **1**, with H atoms omitted for clarity. Color scheme: Mn^{II}, yellow; O, red; C, grey. (For interpretation of the references to colour in this figure legend, the reader is referred to the web version of this article.)

Table 3
Bond valence sum (BVS)^{a, b} calculations for Mn and selected oxygen atoms in **1**

Atom	Mn ^{II}	Mn ^{III}	Mn ^{IV}
Mn1	<u>1.935</u>	1.770	1.858
Mn2	<u>2.023</u>	1.850	1.942
Mn3	<u>2.034</u>	1.860	1.953
	BVS	Assignment	
O1	1.77	OR ⁻ (μ ₃)	
O2	1.97	c	
O3	2.07	c	
O4	1.91	c	
O22	1.85	OR ⁻	

^a The underlined value is the one closest to the charge for which it was calculated. The oxidation state of a particular atom can be taken as the nearest whole number to the underlined value.

^b A BVS in the ~1.8–2.0, ~1.0–1.2 and ~0.2–0.4 ranges for an O atom is indicative of non-, single- and double-protonation, respectively, but can be altered somewhat by hydrogen-bonding.

^c See the corresponding BVS discussion on Section 3.2.

The structure of **1** also contains two strong intramolecular OH...H hydrogen-bonds between one of the MeOH groups and the unbound C=O group of a neighboring EtCO₂ ligand: O(51)...O(22) = 2.482(6) Å. There are no significant intermolecular hydrogen-bonds.

There have been a large number of Mn₆ complexes reported in the literature, most of them being mixed-valent (Mn^{II/III}) or Mn^{III} systems, and these possess a wide variety of metal topologies such as edge-sharing bitetrahedra, octahedra, fused triangles, etc. [19]. However, the only previous example of a Mn₆ cluster with a core consisting of two Mn₃ triangles linked together through a large organic 'spacer' as in **1** was [Mn₆O₂(O₂CPh)₁₂(py)₄(4,4'-bpy)], where 4,4'-bpy acts as the inter-triangle linker [20]. The latter Mn₆ complex has a Mn^{II}Mn₄^{III} oxidation level description, thus leaving **1** as the only example of such a metal topology in Mn^{II} cluster chemistry.

A partially labeled representation and a stereoview of complex **2** are shown in Fig. 4. Selected interatomic distances and angles are

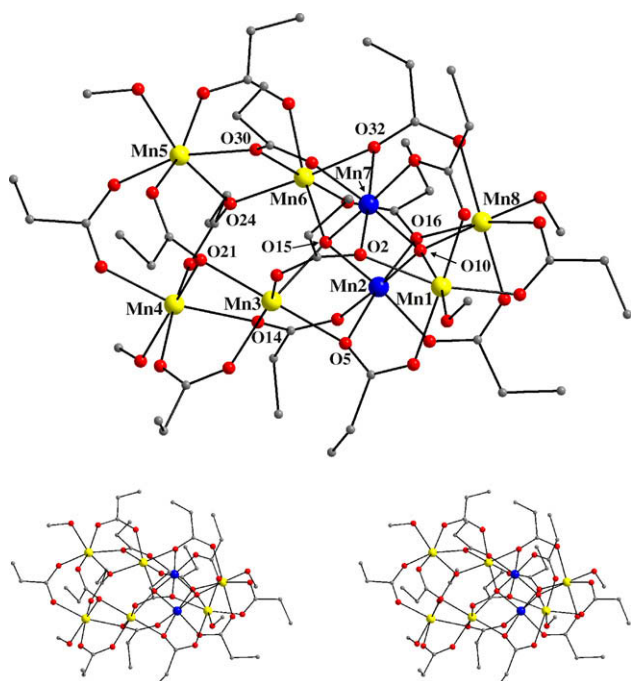


Fig. 4. Labeled PovRay representation (top) and stereopair (bottom) of complex **2**, with H atoms omitted for clarity. Color scheme: Mn^{II}, yellow; Mn^{III}, blue; O, red; C, grey. (For interpretation of the references to colour in this figure legend, the reader is referred to the web version of this article.)

given in Table 4. Complex **2** crystallizes in the orthorhombic space group *Pna2*₁ with the Mn₈ molecule in a general position. The structure consists of a [Mn₈(μ₄-O)₂(μ-OR)₈]⁶⁺ core (Fig. 5, top) which can be considered as an extension of the [Mn₆(μ₄-O)₂(μ-OR)₄]⁶⁺ core of complex **3** (Fig. 5, bottom), and many other similar Mn₆ clusters with a "two edge-sharing tetrahedra" core topology [19b]. In the hexanuclear species, the six O atoms of the core consist of two μ₄-O²⁻ ions with a distorted tetrahedral geometry and four μ-OR⁻ groups from carboxylate ligands. This unit is exactly reproduced in the octanuclear complex **2** and comprises Mn(1,2,3,6,7,8) and O(10,15,2,5,16,32). Extension of this hexanuclear core at one end with two additional Mn atoms, Mn4 and Mn5, each with a bis(μ-OR) bridge from the O atoms of four EtCO₂ ligands to Mn3 and Mn6, respectively, affords the octanuclear core of complex **2**. Peripheral ligation about the core is provided by fourteen EtCO₂ and four terminal MeOH ligands; the latter complete ligation on Mn(1,4,5,8). The 14 EtCO₂ groups are arranged in two classes: (i) six bridge two Mn ions and are in their familiar *syn,syn*-η¹:η¹:μ binding modes, and (ii) eight are in the rare η¹:η²:μ₃ modes, one O bridging two Mn ions and the other O terminal to a third Mn ion, with the bridging carboxylate O atoms being O(2,5,14,16,21,24,30,32).

Charge considerations and an inspection of the metric parameters indicated a 2Mn^{III}, 6Mn^{II} description for **2**. This was confirmed quantitatively by bond valence sum (BVS) calculations (Table 5) [17], which identified Mn2 and Mn7 as the Mn^{III} ions, and the others as Mn^{II}. In addition, the former display Jahn–Teller (JT) axial elongations, typical of high-spin Mn^{III} (d⁴) ions in near-octahedral geometry, with the JT axes avoiding the bridging oxide ions and instead oriented along O5–Mn2–O16 (173.8(2)°) and O2–Mn7–O32 (173.2(2)°). This is an identical arrangement to that observed in **3**.

Table 4
Selected interatomic distances (Å) and bond angles (°) for complex **2**

Interatomic distances			
Mn(1)–O(1)	2.174(7)	Mn(5)–O(22)	2.167(6)
Mn(1)–O(2)	2.305(6)	Mn(5)–O(24)	2.247(6)
Mn(1)–O(4)	2.184(7)	Mn(5)–O(26)	2.217(7)
Mn(1)–O(6)	2.121(7)	Mn(5)–O(27)	2.215(7)
Mn(1)–O(8)	2.152(7)	Mn(5)–O(28)	2.163(6)
Mn(1)–O(10)	2.183(6)	Mn(5)–O(30)	2.226(7)
Mn(2)–O(5)	2.255(6)	Mn(6)–O(15)	2.234(6)
Mn(2)–O(10)	1.895(6)	Mn(6)–O(17)	2.126(6)
Mn(2)–O(11)	1.963(6)	Mn(6)–O(24)	2.131(6)
Mn(2)–O(13)	1.966(6)	Mn(6)–O(29)	2.148(6)
Mn(2)–O(15)	1.902(6)	Mn(6)–O(30)	2.227(6)
Mn(2)–O(16)	2.207(6)	Mn(6)–O(32)	2.203(6)
Mn(3)–O(3)	2.117(7)	Mn(7)–O(2)	2.218(6)
Mn(3)–O(5)	2.211(6)	Mn(7)–O(9)	1.943(7)
Mn(3)–O(14)	2.246(7)	Mn(7)–O(10)	1.883(6)
Mn(3)–O(15)	2.269(6)	Mn(7)–O(15)	1.908(6)
Mn(3)–O(18)	2.126(8)	Mn(7)–O(31)	1.995(7)
Mn(3)–O(21)	2.169(7)	Mn(7)–O(32)	2.184(6)
Mn(4)–O(14)	2.218(6)	Mn(8)–O(7)	2.159(7)
Mn(4)–O(19)	2.124(7)	Mn(8)–O(10)	2.196(6)
Mn(4)–O(20)	2.226(7)	Mn(8)–O(12)	2.144(7)
Mn(4)–O(21)	2.251(7)	Mn(8)–O(16)	2.269(6)
Mn(4)–O(23)	2.172(7)	Mn(8)–O(33)	2.175(7)
Mn(4)–O(25)	2.137(6)	Mn(8)–O(34)	2.191(7)
Bond angles			
Mn(1)–O(2)–Mn(7)	88.0(2)	Mn(2)–O(16)–Mn(8)	90.0(2)
Mn(1)–O(10)–Mn(2)	119.7(3)	Mn(3)–O(14)–Mn(4)	97.7(3)
Mn(1)–O(10)–Mn(7)	100.9(3)	Mn(3)–O(15)–Mn(6)	126.9(3)
Mn(1)–O(10)–Mn(8)	118.7(3)	Mn(3)–O(15)–Mn(7)	116.9(3)
Mn(2)–O(5)–Mn(3)	91.5(2)	Mn(3)–O(21)–Mn(4)	99.0(3)
Mn(2)–O(10)–Mn(7)	96.2(3)	Mn(5)–O(24)–Mn(6)	99.9(3)
Mn(2)–O(10)–Mn(8)	101.1(3)	Mn(5)–O(30)–Mn(6)	97.6(3)
Mn(2)–O(15)–Mn(3)	99.8(3)	Mn(6)–O(15)–Mn(7)	98.2(3)
Mn(2)–O(15)–Mn(6)	116.2(3)	Mn(6)–O(32)–Mn(7)	91.4(2)
Mn(2)–O(15)–Mn(7)	95.2(3)	Mn(7)–O(10)–Mn(8)	118.9(3)

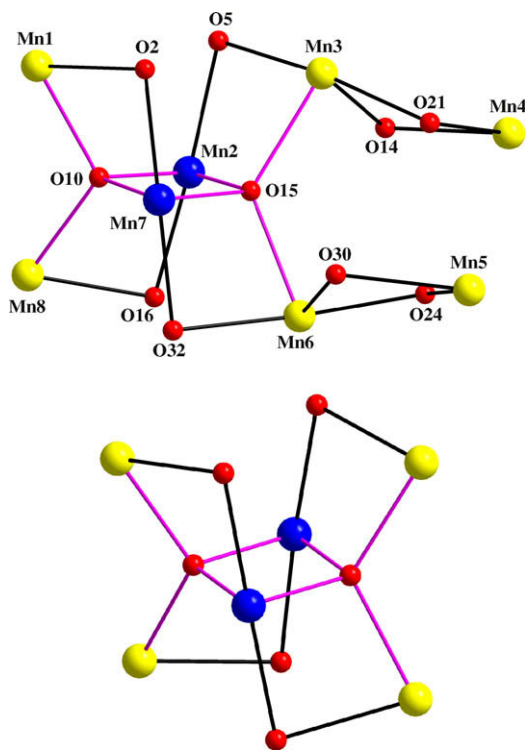


Fig. 5. Labeled PovRay representation of (top) the complete $[\text{Mn}_8(\mu_4\text{-O})_2(\mu\text{-OR})_8]^{6+}$ core of **2**, and (bottom) the $[\text{Mn}_6(\mu_4\text{-O})_2(\mu\text{-OR})_4]^{6+}$ core of complex **3** emphasizing in both cases the “two edge-sharing tetrahedra” $[\text{Mn}_6(\mu_4\text{-O})_2]^{10+}$ subcore (purple thick lines). Color scheme: Mn^{II} , yellow; Mn^{III} , blue; O, red; C, grey. (For interpretation of the references to colour in this figure legend, the reader is referred to the web version of this article.)

Table 5
Bond valence sums for Mn^{a} and selected oxygen^b atoms in complex **2**

Atom	Mn^{II}	Mn^{III}	Mn^{IV}
Mn1	1.942	1.777	1.865
Mn2	3.130	2.863	3.005
Mn3	1.927	1.763	1.850
Mn4	1.928	1.764	1.852
Mn5	1.921	1.757	1.844
Mn6	1.979	1.810	1.900
Mn7	3.178	2.907	3.052
Mn8	1.918	1.755	1.842
	BVS	Assignment	
O10	1.84	$\text{O}^{2-}(\mu_4)$	
O15	1.70	$\text{O}^{2-}(\mu_4)$	

^a See footnote a of Table 3.

^b See footnote b of Table 3.

All the Mn^{II} atoms are also six-coordinate with distorted octahedral geometries. The protonation level of O^{2-} groups (O10 and O15) was also confirmed by BVS calculations (Table 5). Furthermore, although there is no crystallographic symmetry, the core of **2** possesses a virtual C_2 axis, passing through O10 and O15. Finally, the structure contains four strong intermolecular $\text{OH} \cdots \text{H}$ hydrogen-bonds between the four MeOH OH groups and four of the bridging EtCO_2^- in neighboring molecules ($\text{O1} \cdots \text{O28} = 2.708(3)$ Å, $\text{O20} \cdots \text{O7} = 2.702(3)$ Å, $\text{O27} \cdots \text{O4} = 2.765(3)$ Å, $\text{O34} \cdots \text{O25} = 2.709(3)$ Å).

Complex **2** joins only a small family of Mn clusters of nuclearity eight, which currently comprise the metal oxidation states Mn_8^{II} [21], $\text{Mn}_6^{\text{II}}\text{Mn}_2^{\text{III}}$ [22], $\text{Mn}_4^{\text{II}}\text{Mn}_4^{\text{III}}$ [23,6b], $\text{Mn}_2^{\text{II}}\text{Mn}_6^{\text{III}}$ [24], Mn_8^{III} [25] and $\text{Mn}_2^{\text{III}}\text{Mn}_6^{\text{IV}}$ [26], and thus becomes the third member of the $\text{Mn}_6^{\text{II}}\text{Mn}_2^{\text{III}}$ subfamily. The $[\text{Mn}_8\text{O}_{10}]$ core of **2** is similar to that in the $[\text{Mn}_8\text{O}_2(\text{O}_2\text{CCH}_2\text{Bu}^t)_4(\text{Bu}^t\text{CH}_2\text{CO}_2\text{H})_4]$ carboxylato cluster [22b].

3.3. Magnetochemistry

3.3.1. Magnetic susceptibility studies of complex **1**

Variable-temperature magnetic susceptibility measurements were performed on a powdered polycrystalline sample of complex **1**, restrained in eicosane to prevent torquing, in a 1 kG (0.1 T) field and in the 5.0–300 K range. The data are shown as a $\chi_{\text{M}}T$ vs T plot in Fig. 6 (top). The $\chi_{\text{M}}T$ value of $24.24 \text{ cm}^3 \text{ Kmol}^{-1}$ at 300 K decreases gradually with decreasing temperature to $3.72 \text{ cm}^3 \text{ Kmol}^{-1}$ at 5.0 K. The 300 K value is appreciably less than the spin-only ($g = 2$) value of $26.25 \text{ cm}^3 \text{ Kmol}^{-1}$ for six Mn^{II} non-interacting ions, indicating the presence of dominant antiferromagnetic exchange interactions and suggesting a low, but non-zero, ground state S value. The 5.0 K value is consistent with an $S = 5/2$ ground state, with a g factor slightly less than 2.0; the spin-only value for $S = 5/2$ is $4.375 \text{ cm}^3 \text{ Kmol}^{-1}$.

Due to the large separation between the two identical Mn_3^{II} triangular subunits within **1** induced by the octadentate ligand L, and the expected negligible exchange interaction between them, we fit the data assuming two non-interacting $[\text{Mn}_3(\mu_3\text{-OR})(\mu\text{-OR})_2]^{3+}$ (Fig. 6, bottom) units. In order to determine the individual pairwise exchange parameters J_{ij} between Mn_iMn_j pairs within each Mn_3 unit, the $\chi_{\text{M}}T$ vs T data were fit to the appropriate theoretical expression for a Mn_3^{II} isosceles triangle. The isosceles model requires two exchange parameters, and the resulting isotropic Heisenberg spin Hamiltonian is given by Eq. (2), where $J = J_{12} = J_{13}$ and $J' = J_{23}$ refer to the $\text{Mn}^{\text{II}}\text{Mn}^{\text{II}}$ exchange interactions of a C_{2v} symmetry isosceles triangle, with Mn2–Mn3 being the unique edge.

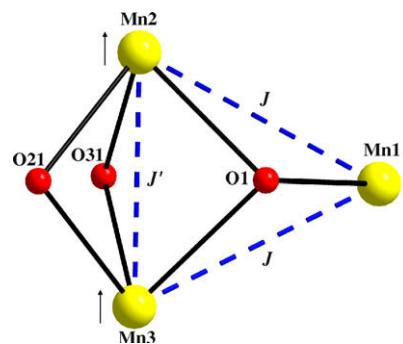
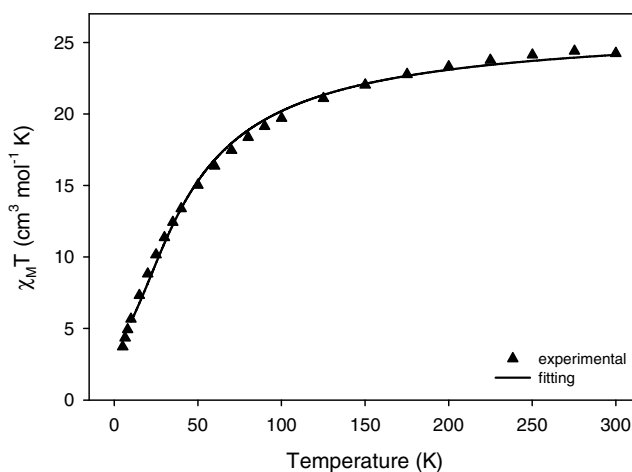


Fig. 6. (top) Plot of $\chi_{\text{M}}T$ vs T for complex **1**. The solid line is the fit of the data; see the text for the fit parameters. (bottom) Labeled PovRay representation of the $[\text{Mn}_3(\mu_3\text{-OR})(\mu\text{-OR})_2]^{3+}$ core of each Mn_3 subunit of **1**, emphasizing the spin alignments that give the observed $S = 5/2$ ground state (see text). Color scheme: Mn^{II} , yellow; O, red. (For interpretation of the references to colour in this figure legend, the reader is referred to the web version of this article.)

$$\mathcal{H} = -2J(\hat{S}_1 \cdot \hat{S}_2 + \hat{S}_1 \cdot \hat{S}_3) - 2J'\hat{S}_2 \cdot \hat{S}_3 \quad (2)$$

Applying the Kambe approach [27] using the substitutions $\hat{S}_A = \hat{S}_2 + \hat{S}_3$ and $\hat{S}_T = \hat{S}_A + \hat{S}_1$, where S_T is the total spin of the whole molecule, gives the equivalent spin Hamiltonian of Eq. (3).

$$\mathcal{H} = -J(\hat{S}_T^2 - \hat{S}_A^2 - \hat{S}_1^2) - J'(\hat{S}_A^2 - \hat{S}_2^2 - \hat{S}_3^2) \quad (3)$$

The eigenvalues of Eq. (3) are given by Eq. (4), where $E(S_T, S_A)$ is the energy of state S_T arising from S_A , and constant terms contributing to all states have been omitted. For complex **1**, $S_1 = S_2 = S_3 = 5/2$, and the overall multiplicity of the spin system is 216, made up of 58 individual spin states ranging from $S_T = 1/2$ – $15/2$.

$$E(S_T, S_A) = -J[S_T(S_T + 1) - S_A(S_A + 1)] - J'[S_A(S_A + 1)] \quad (4)$$

A theoretical $\chi_M T$ vs T expression was derived using the S_T values, their energies $E(S_T)$, and the Van Vleck equation, and this expression was used to fit the experimental data. Data below 10 K were omitted because the low-temperature decrease is caused by factors not included in the above model. The fit parameters were J , J' and g . A temperature-independent paramagnetism (TIP) term was included, held fixed at $600 \times 10^{-6} \text{ cm}^3 \text{ mol}^{-1}$. The obtained good fit (solid line in Fig. 6 (top)) gave $J = -2.04(3) \text{ cm}^{-1}$, $J' = +0.79(3)$, and $g = 1.98(5)$. Thus, there are both ferro- and antiferromagnetic exchange interactions within **1** giving an $S_T = 5/2$ ground state, the $|S_T, S_A \rangle = |5/2, 5 \rangle$ state, and a $|S_T, S_A \rangle = |3/2, 4 \rangle$ first excited state at 10.20 cm^{-1} above the ground state; the second excited state is the $|S_T, S_A \rangle = |7/2, 5 \rangle$ which lies 14.28 cm^{-1} above the ground state. Both J and J' are relatively weak, as typically expected for $\text{Mn}^{\text{II}}\text{--Mn}^{\text{II}}$ exchange interactions promoted by oxide and/or alkoxide groups [28].

The $S_T = 5/2$ ground state is the expected one, given the fact that one of the exchange interactions is ferromagnetic (J') whereas the other one is antiferromagnetic (J); thus, no spin frustration effects are operative (Fig. 6, bottom). Moreover, such a spin ground state value can also be rationalized according to previous magnetostructural correlations reported for many Mn_x^{II} complexes [28]. In particular, (i) it is expected that μ_3 -bridging oxide groups give weak antiferromagnetic $\text{Mn}^{\text{II}}\text{--Mn}^{\text{II}}$ interactions, and (ii) tris-monoatomically bridging by an oxide (O1) and two OR^- (O21, O31) of Mn^{II} ions such as Mn_2/Mn_3 with corresponding and relatively acute angles of $86.8(1)$, $86.8(1)$ and $88.4(1)^\circ$, respectively, will likely result in ferromagnetic coupling.

To confirm the indicated $S = 5/2$ ground state of **1** and to determine D , magnetization data were collected in the magnetic field and temperature ranges 1–70 kG and 1.8–10.0 K. However, we could not get an acceptable fit using data collected over the whole field range, which is a common problem caused by low-lying excited states, especially if some have an S value greater than that of the ground state, as is the case for **1**. A common solution is to only use data collected with low fields ($\leq 1.0 \text{ T}$), as we previously reported for many Mn^{II} and/or mixed-valence $\text{Mn}^{\text{II}}/\text{Mn}^{\text{III}}$ clusters [29]. However, it was still not possible to obtain a satisfactory fit assuming that only the ground state is populated in this temperature range. This suggests that low-lying excited states are populated, even at these relatively low temperatures.

Thus, in an additional effort to confirm the spin ground state of each Mn_3^{II} subunits of complex **1**, we turned to ac susceptibility measurements in a 3.5 G ac field oscillating at frequencies in the 50–1000 Hz range. As we have described before on multiple occasions [10,11,29], ac susceptibility studies are a powerful complement to dc studies for determining the ground state of a system, because they preclude any complications arising from the presence of a dc field. The in-phase $\chi_M T$ vs T data are shown in Fig. 7 and show a rapid decrease below 10 K consistent with decreasing population of low-lying excited states with S greater than that of the ground state. The plot from above $\sim 6 \text{ K}$ extrapolate to just over $\chi_M T \sim 4$ at 0 K, which is consistent with an $S = 5/2$ ground state,

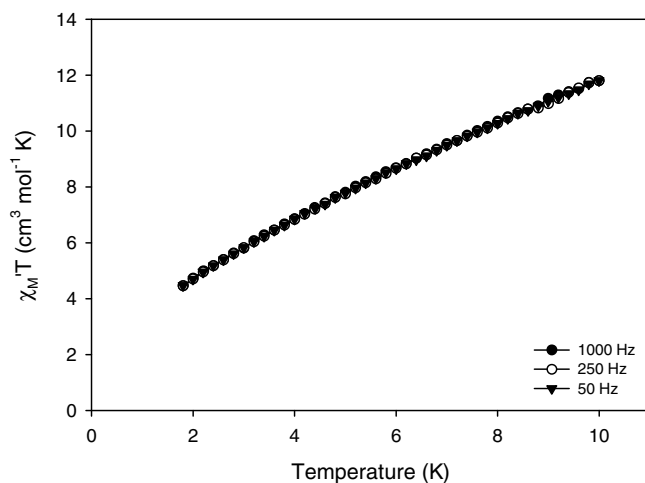


Fig. 7. Plot of the in-phase ac susceptibility signals, $\chi_M T$ vs T for complex **1** (per Mn_3 subunit) at the indicated frequencies.

in satisfying agreement with the dc fit. Below 6 K, the data begin to decrease very slightly faster, which is probably due to very weak interactions between the two Mn_3 units within **1**. As expected, due to the minimal single-ion anisotropy of the Mn^{II} ions and the relatively small spin ground state value of the cluster, there were no out-of-phase ac signals down to 1.8 K.

3.3.2. Magnetic susceptibility studies of complex 2

Variable-temperature magnetic susceptibility measurements were performed on a microcrystalline powder sample of **2**, restrained in eicosane to prevent torquing, in a 1 kG (0.1 T) field and in the 5.0–300 K range. The obtained data are shown as a $\chi_M T$ vs T plot in Fig. 8. The $\chi_M T$ value of $28.62 \text{ cm}^3 \text{ K mol}^{-1}$ at 300 K decreases gradually with decreasing temperature to $3.42 \text{ cm}^3 \text{ K mol}^{-1}$ at 5.0 K. Again, the 300 K value is much less than the spin-only ($g = 2$) value of $32.25 \text{ cm}^3 \text{ K mol}^{-1}$ for six Mn^{II} and two Mn^{III} non-interacting ions, indicating the presence of dominant antiferromagnetic exchange interactions and strongly suggesting a low, probably zero, ground state S value. Owing to the size and low symmetry of the molecule, it is not possible to apply the Kambe method [27] or otherwise evaluate the exchange parameters between the Mn ions. However, the $S = 0$ ground state was further supported by the ac in-phase $\chi_M T$ vs T data (Fig. 9), which show a steady decrease below 10 K and are clearly heading for $\chi_M T \sim 0$ at 0 K.

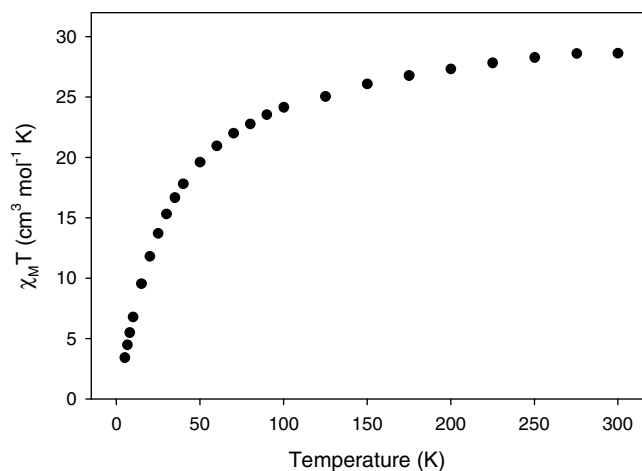


Fig. 8. Plot of $\chi_M T$ vs T for complex **2**.

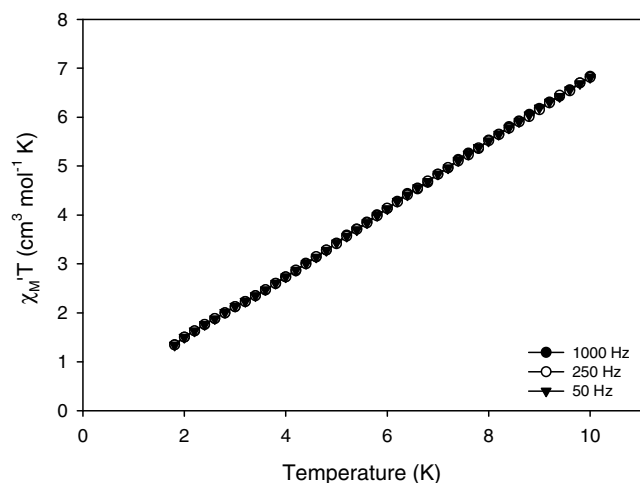


Fig. 9. Plot of the in-phase ac susceptibility signals, $\chi_M''T$ vs T for complex **2** at the indicated frequencies.

The $S = 0$ spin ground state for **2** can be rationalized by considering its structural relationship to the family of compounds of formula $[\text{Mn}_6\text{O}_2(\text{O}_2\text{CPh})_{10}(\text{L}')_4]$ ($\text{L}' = \text{py}, \text{MeCN}, \text{H}_2\text{O}/\text{PhCO}_2\text{H}$ (**3**)) [19a,19b,19c,19d,19e,19f,19g,19h]. In the latter complexes, such as **3**, the most dominant exchange interaction is the antiferromagnetic one ($J = -42 \text{ cm}^{-1}$) between the bis(μ -O)-bridged Mn^{III} centers, which results in an overall $S = 0$ ground state whatever the spins of each of the two halves of the molecule might be [19g]. The $[\text{Mn}_2^{\text{II}}\text{Mn}_2^{\text{III}}\text{O}_2]^{10+}$ core of complex **3** is essentially preserved in **2**, which differs only by the presence of two additional peripheral Mn^{II} centers. Typically, $\text{Mn}^{\text{II}}-\text{Mn}^{\text{II}}$ and $\text{Mn}^{\text{II}}-\text{Mn}^{\text{III}}$ exchange interactions are weak and antiferromagnetic [28,30]. Hence, the dominant exchange interaction is again likely to be an antiferromagnetic one between Mn^{II} and Mn^{III} through the carboxylate groups bridging them, resulting in the observed $S = 0$ ground state for the complex.

4. Conclusions and perspectives

The initial use of thbH_3 in Mn carboxylate chemistry has generally revealed its instability to redox transformations in the presence of *in situ* generated Mn^{III} . Nevertheless, it has provided access to new Mn^{II} and $\text{Mn}^{\text{II/III}}$ carboxylate clusters spanning Mn_6 and Mn_8 nuclearities and topologies that are either prototypical or very rare, respectively. The thbH_3 group has undoubtedly undergone the same redox transformation in both reaction systems, and its occurrence as a bridging octadentate ligand L^{4-} in $[\text{Mn}_6(\text{O}_2\text{C}_2\text{Et})_8(\text{L})(\text{MeOH})_4(\text{H}_2\text{O})_2]$ (**1**) has fortunately allowed its identification.

Our future work will be oriented towards the further investigation of deprotonated thbH_3 and its transformed versions as a potentially multidentate ligand in Mn chemistry, as well as with other transition metals, particularly those that are less oxidizing. In addition, there are other aromatic poly-ols whose reactions would make for interesting comparisons with those of thbH_3 . It will be particularly interesting to extend this work to Fe^{III} , which has a strong preference for aromatic alcohols such as phenol and catechol.

Acknowledgement

This work was supported by NSF (CHE-0414555 to G.C.).

Appendix A. Supplementary data

PovRay representation of the completely labeled core of complex **1** (Fig. S1). Crystallographic data in CIF format have been

deposited at the Cambridge Crystallographic Data Centre with CCDC Nos. 675212 (**1**), 675214 (**2**) and 675213 (**3**). Copies of this information may be obtained free of charge from The Director, CCDC, 12 Union Road, Cambridge, CB2 1EZ, UK (fax: +44 1223 336033; e-mail: deposit@ccdc.cam.ac.uk or <http://www.ccdc.cam.ac.uk>). Supplementary data associated with this article can be found in the online version, at doi:10.1016/j.molstruc.2008.04.031.

References

- [1] (a) K.N. Ferreira, T.M. Iverson, K. Maghlaoui, J. Barber, S. Iwata, *Science* 303 (2004) 1831; (b) T.G. Carrell, A.M. Tyryshkin, G.C. Dismukes, *J. Biol. Inorg. Chem.* 7 (2002) 2; (c) R.M. Cinco, A. Rompel, H. Visser, G. Aromi, G. Christou, K. Sauer, M.P. Klein, V.K. Yachandra, *Inorg. Chem.* 38 (1999) 5988; (d) V.K. Yachandra, K. Sauer, M.P. Klein, *Chem. Rev.* 96 (1996) 2927; (e) N.A. Law, M.T. Caudle, V.L. Pecoraro, in: A.G. Sykes (Ed.), *Advances in Inorganic Chemistry*, vol. 46, Academic Press, London, 1998, p. 305; (f) C.F. Yocum, V.L. Pecoraro, *Curr. Opin. Chem. Biol.* 3 (1999) 182.
- [2] For some representative references, see: (a) G. Christou, D. Gatteschi, D.N. Hendrickson, R. Sessoli, *MRS Bull.* 25 (2000) 66; (b) R. Sessoli, H.-L. Tsai, A.R. Schake, S. Wang, J.B. Vincent, K. Folting, D. Gatteschi, G. Christou, D.N. Hendrickson, *J. Am. Chem. Soc.* 115 (1993) 1804.
- [3] (a) R. Bircher, G. Chaboussant, D. Dobe, H.U. Güdel, S.T. Oshensbein, A. Sieber, O. Waldmann, *Adv. Funct. Mater.* 16 (2006) 209; (b) D. Gatteschi, R. Sessoli, *Angew. Chem. Int. Ed.* 42 (2003) 268; (c) S.M.J. Aubin, N.R. Gilley, L. Pardi, J. Krzystek, M.W. Wemple, L.-C. Brunel, M.B. Maple, G. Christou, D.N. Hendrickson, *J. Am. Chem. Soc.* 120 (1998) 4991; (d) H. Oshio, M. Nakano, *Chem. Eur. J.* 11 (2005) 5178.
- [4] For some representative references, see: (a) D. Arndt, *Manganese Compounds as Oxidizing Agents in Organic Chemistry*, Open Court Publishing Company, Illinois, USA, 1981; (b) B.B. Snider, *Chem. Rev.* 96 (1996) 339; (c) T.-L. Ho, in: W.J. Mijs, C.R.H.I. de Jonge (Eds.), *Organic Syntheses By Oxidation With Metal Compounds*, Plenum, New York, 1986, Chapter 11, pp. 569–631.; (d) A.J. Tasiopoulos, T.A. O'Brien, K.A. Abboud, G. Christou, *Angew. Chem. Int. Ed.* 43 (2004) 345. and references therein.
- [5] For a mini-review describing the available synthetic procedures to Mn carboxylate SMMs, see: G. Christou, *Polyhedron* 24 (2005) 2065. and references therein.
- [6] (a) G. Aromi, S.M.J. Aubin, M.A. Bolcar, G. Christou, H.J. Eppley, K. Folting, D.N. Hendrickson, J.C. Huffman, R.C. Squire, H.-L. Tsai, S. Wang, M.W. Wemple, *Polyhedron* 17 (1998) 3005. and references therein; (b) M. Murugesu, W. Wernsdorfer, K.A. Abboud, G. Christou, *Angew. Chem. Int. Ed.* 44 (2005) 892. and references therein; (c) D. Foguet-Albiol, T.A. O'Brien, W. Wernsdorfer, B. Moulton, M.J. Zaworotko, K.A. Abboud, G. Christou, *Angew. Chem. Int. Ed.* 44 (2005) 897; (d) Th. C. Stamatatos, D. Foguet-Albiol, S.P. Perlepes, C.P. Raptopoulou, A. Terzis, C.S. Patrickios, G. Christou, A.J. Tasiopoulos, *Polyhedron* 25 (2006) 1737; (e) Th. C. Stamatatos, B. Luisi, B. Moulton, G. Christou, *Inorg. Chem.* 47 (2008) 1134; (f) Th. C. Stamatatos, D. Foguet-Albiol, C.C. Stoumpos, C.P. Raptopoulou, A. Terzis, W. Wernsdorfer, S.P. Perlepes, G. Christou, *J. Am. Chem. Soc.* 127 (2005) 15380; (g) Th. C. Stamatatos, D. Foguet-Albiol, S.-C. Lee, C.C. Stoumpos, C.P. Raptopoulou, A. Terzis, W. Wernsdorfer, S. Hill, S.P. Perlepes, G. Christou, *J. Am. Chem. Soc.* 129 (2007) 9484; (h) R. Bagai, K.A. Abboud, G. Christou, *Inorg. Chem.* 47 (2008) 621.
- [7] For example, see: (a) J.B. Vincent, C. Christmas, H.-R. Chang, Q. Li, P.D.W. Boyd, J.C. Huffman, D.N. Hendrickson, G. Christou, *J. Am. Chem. Soc.* 111 (1989) 2086; (b) A.J. Tasiopoulos, K.A. Abboud, G. Christou, *Chem. Commun.* (2003) 580.
- [8] E. Libby, J.K. McCusker, E.A. Schmitt, K. Folting, D.N. Hendrickson, G. Christou, *Inorg. Chem.* 30 (1991) 3486.
- [9] For example, see: (a) S. Wang, H.-L. Tsai, E. Libby, K. Folting, W.E. Streib, D.N. Hendrickson, G. Christou, *Inorg. Chem.* 35 (1996) 7578; (b) G. Aromi, M.J. Knapp, J.-P. Claude, J.C. Huffman, D.N. Hendrickson, G. Christou, *J. Am. Chem. Soc.* 121 (1999) 5489.
- [10] (a) Th. C. Stamatatos, K.A. Abboud, W. Wernsdorfer, G. Christou, *Angew. Chem. Int. Ed.* 46 (2007) 884; (b) M. Murugesu, M. Habrych, W. Wernsdorfer, K.A. Abboud, G. Christou, *J. Am. Chem. Soc.* 126 (2004) 4766; (c) E.K. Brechin, J. Yoo, J.C. Huffman, D.N. Hendrickson, G. Christou, *Chem. Commun.* (1999) 783; (d) M. Murugesu, W. Wernsdorfer, K.A. Abboud, G. Christou, *Polyhedron* 24 (2005) 2894; (e) H. Miyasaka, K. Nakata, L. Lecren, C. Coulon, Y. Nakazawa, T. Fujisaki, K. Sugiura, M. Yamashita, R. Clérac, *J. Am. Chem. Soc.* 128 (2006) 3770; (f) M. Murugesu, A. Mishra, W. Wernsdorfer, K.A. Abboud, G. Christou, *Polyhedron* 25 (2006) 613; (g) N.C. Harden, M.A. Bolcar, W. Wernsdorfer, K.A. Abboud, W.E. Streib, G. Christou, *Inorg. Chem.* 42 (2003) 7067;

- (h) C. Boskovic, E.K. Brechin, W.E. Streib, K. Folting, J.C. Bollinger, D.N. Hendrickson, G. Christou, *J. Am. Chem. Soc.* 124 (2002) 3725;
- (i) L. Lecren, O. Roubeau, C. Coulon, Y.-G. Li, X.F.L. Goff, W. Wernsdorfer, H. Miyasaka, R. Clérac, *J. Am. Chem. Soc.* 127 (2005) 17353;
- (j) L. Lecren, W. Wernsdorfer, Y.-G. Li, O. Roubeau, H. Miyasaka, R. Clérac, *J. Am. Chem. Soc.* 127 (2005) 11311;
- (k) Th. C. Stamatatos, K.A. Abboud, W. Wernsdorfer, G. Christou, *Angew. Chem. Int. Ed.* 45 (2006) 4134;
- (l) Th. C. Stamatatos, K.A. Abboud, W. Wernsdorfer, G. Christou, *Polyhedron* 26 (2007) 2042.
- [11] (a) E. Moushi, Th. C. Stamatatos, W. Wernsdorfer, V. Nastopoulos, G. Christou, A.J. Tasiopoulos, *Angew. Chem. Int. Ed.* 45 (2006) 7722;
- (b) E. Moushi, C. Lampropoulos, W. Wernsdorfer, V. Nastopoulos, G. Christou, A.J. Tasiopoulos, *Inorg. Chem.* 46 (2007) 3795.
- [12] For a recent review, see: E.K. Brechin, *Chem. Commun.* (2005) 5141. and references therein.
- [13] For a representative review, see: R.E.P. Winpenny, *J. Chem. Soc. Dalton Trans.* (2002) 1. and references therein.
- [14] C. Cañada-Vilalta, T.A. O'Brien, M. Pink, E.R. Davidson, G. Christou, *Inorg. Chem.* 42 (2003) 7819.
- [15] G. Aromi, S. Bhaduri, P. Artús, J.C. Huffman, D.N. Hendrickson, G. Christou, *Polyhedron* 21 (2002) 1779.
- [16] SHELXTL6; Bruker-AXS, Madison, WI, 2000.
- [17] (a) I.D. Brown, D. Altermatt, *Acta Crystallogr. B* 41 (1985) 244;
- (b) W. Liu, H.H. Thorp, *Inorg. Chem.* 32 (1993) 4102.
- [18] For example, see: (a) S. Schoumacker, O. Hamelin, J. Pecaut, M. Fontecave, *Inorg. Chem.* 42 (2003) 8110;
- (b) S. Shibata, S. Onuma, H. Inoue, *Chem. Lett.* (1984) 485;
- (c) F.S. Stephens, *Acta Crystallogr. Sect. B* 33 (1977) 3492;
- (d) S. Muhammad, M. Mazhar, M. Zeller, A.D. Hunter, *Acta Crystallogr. Sect. E* 62 (2006) m224;
- (e) R. van Gorkum, F. Buda, H. Kooijman, A.L. Spek, E. Bouwman, J. Reedijk, *Eur. J. Inorg. Chem.* (2005) 2255.
- [19] (a) D.M. Low, E.K. Brechin, M. Helliwell, T. Mallah, E. Riviere, E.J.L. McInnes, *Chem. Commun.* (2003) 2330;
- (b) M.A. Halcrow, W.E. Streib, K. Folting, G. Christou, *Acta Crystallogr. Sect. C* 51 (1995) 1263;
- (c) M. Murie, S. Parsons, R.E.P. Winpenny, *J. Chem. Soc. Dalton Trans.* (1998) 1423;
- (d) A.R.E. Baikie, A.J. Howes, M.B. Hursthouse, A.B. Quick, P.J. Thornton, *J. Chem. Soc. Chem. Commun.* (1986) 1587;
- (e) A.S. Batsanov, Y.T. Struchkov, G.A. Timco, N.V. Gerbeleu, O.S. Manole, S.V. Grebenko, *Russ. J. Coord. Chem.* 20 (1994) 604;
- (f) A.G. Blackman, J.C. Huffman, E.B. Lobkovsky, G. Christou, *Polyhedron* 11 (1992) 251;
- (g) A.R. Schake, J.B. Vincent, Q. Li, P.D.W. Boyd, K. Folting, J.C. Huffman, D.N. Hendrickson, G. Christou, *Inorg. Chem.* 28 (1989) 1915;
- (h) K.S. Gavrilenko, S.V. Punin, O. Cadot, S. Golhen, L. Quahab, V.V. Pavlishchuk, *Inorg. Chem.* 44 (2005) 5903;
- (i) C.J. Milios, S. Piligkos, E.K. Brechin, *Dalton Trans.* (2008) 1809.
- [20] H.J. Eppley, N. deVries, S. Wang, S.M. Aubin, H.-L. Tsai, K. Folting, D.N. Hendrickson, G. Christou, *Inorg. Chim. Acta* 263 (1997) 323.
- [21] For example, see: (a) R.W. Saalfrank, N. Löw, B. Demleitner, D. Stalke, M. Teichert, *Chem. Eur. J.* 4 (1998) 1305;
- (b) R.W. Saalfrank, N. Löw, S. Trummer, G.M. Sheldrick, M. Teichert, D. Stalke, *Eur. J. Inorg. Chem.* (1998) 559.
- [22] (a) C. Boskovic, W. Wernsdorfer, K. Folting, J.C. Huffman, D.N. Hendrickson, G. Christou, *Inorg. Chem.* 41 (2002) 5107;
- (b) C. Boskovic, J.C. Huffman, G. Christou, *Chem. Commun.* (2002) 2502.
- [23] (a) C.J. Milios, Th. C. Stamatatos, P. Kyritsis, A. Terzis, C.P. Raptopoulou, R. Vicente, A. Escuer, S.P. Perlepes, *Eur. J. Inorg. Chem.* (2004) 2885;
- (b) C.J. Milios, F.P.A. Fabbiani, S. Parsons, M. Murugesu, G. Christou, E.K. Brechin, *Dalton Trans.* (2006) 351.
- [24] (a) M.W. Wemple, H.-L. Tsai, S. Wang, J.P. Claude, W.E. Streib, J.C. Huffman, D.N. Hendrickson, G. Christou, *Inorg. Chem.* 35 (1996) 6437;
- (b) C.J. Milios, R. Inglis, A. Vinslava, A. Prescimone, S. Parsons, S.P. Perlepes, G. Christou, E.K. Brechin, *Inorg. Chem.* 46 (2007) 6215.
- [25] For some representative references, see: (a) E. Libby, K. Folting, C.J. Huffman, J.C. Huffman, G. Christou, *Inorg. Chem.* 32 (1993) 2549;
- (b) E.K. Brechin, M. Soler, G. Christou, M. Helliwell, S.J. Teat, W. Wernsdorfer, *Chem. Commun.* (2003) 1276;
- (c) V.A. Grillo, M.J. Knapp, J.C. Bollinger, D.N. Hendrickson, G. Christou, *Angew. Chem. Int. Ed.* 35 (1996) 1818;
- (d) S. Tanase, G. Aromi, E. Bouwman, H. Kooijman, A.L. Spek, J. Reedijk, *Chem. Commun.* (2005) 3147.
- [26] A.J. Tasiopoulos, K.A. Abboud, G. Christou, *Chem. Commun.* (2003) 580.
- [27] K. Kambe, *J. Phys. Soc. Jpn.* 5 (1950) 48.
- [28] O. Kahn, *Molecular Magnetism*, VCH Publishers, New York, 1993.
- [29] (a) M. Soler, W. Wernsdorfer, K. Folting, M. Pink, G. Christou, *J. Am. Chem. Soc.* 126 (2004) 2156;
- (b) E.K. Brechin, E.C. Sanudo, W. Wernsdorfer, C. Boskovic, J. Yoo, D.N. Hendrickson, A. Yamaguchi, H. Ishimoto, T.E. Concolino, A.L. Rheingold, G. Christou, *Inorg. Chem.* 44 (2005) 502;
- (c) P. King, W. Wernsdorfer, K.A. Abboud, G. Christou, *Inorg. Chem.* 44 (2005) 8659;
- (d) A.J. Tasiopoulos, W. Wernsdorfer, K.A. Abboud, G. Christou, *Inorg. Chem.* 44 (2005) 6324.
- [30] Th. C. Stamatatos, G. Christou, *Phil. Trans. R. Soc. A* (2007), doi:10.1098/rsta.2007.214. and references therein.